

Appearance of a new phase across the T_d - $1T'$ phase boundary in Weyl semimetal MoTe_2

Yu Tao,¹ John A. Schneeloch,¹ Chunruo Duan,¹ Masaaki Matsuda,² Sachith E. Dissanayake,^{2,*} Adam A. Aczel,^{2,3} Jaime A. Fernandez-Baca,² Feng Ye,² and Despina Louca^{1,†}

¹*Department of Physics, University of Virginia, Charlottesville, Virginia 22904, USA*

²*Neutron Scattering Division, Oak Ridge National Laboratory, Oak Ridge, Tennessee 37831, USA*

³*Department of Physics and Astronomy, University of Tennessee, Knoxville, Tennessee 37996, USA*

Using elastic neutron scattering on single crystals of MoTe_2 , we show that a new phase appears on warming from the low-temperature orthorhombic T_d phase to the high-temperature monoclinic $1T'$ phase. The new phase, which we refer to as T_d^* , consists of four layers rather than two in its unit cell, and is constructable by an “AABB” sequence of stacking operations rather than “AB” and “AA” for the $1T'$ and T_d phases, respectively. The T_d^* phase emerges without disorder on warming from T_d , though further warming is accompanied by diffuse scattering indicating stacking disorder, which dissipates as the crystal warms further into $1T'$. On cooling, diffuse scattering is observed that suggests a frustrated tendency toward the “AABB” stacking.

Many layered materials have structure-property relationships that depend on their layer stacking. For example, the transition metal dichalcogenide MoTe_2 is reported to be a type-II Weyl semimetal in its orthorhombic T_d phase [1, 2] but not in its monoclinic $1T'$ phase, even though these phases have nearly-identical layers and differ mainly in the in-plane displacements that occur when $1T'$ is cooled into T_d . Though there is much interest in investigating Weyl semimetals, the properties of MoTe_2 are not completely clear. For instance, there is much debate on the origin of the extreme magnetoresistance seen at low temperatures [3–5], the number and locations of Weyl points in the T_d phase [6], and the topological nature of observed surface Fermi arcs that are a necessary but not a sufficient condition for a Weyl semimetal [7]. Structural distortions have been known to occur, such as stacking disorder during the phase transition, evidenced by the presence of diffuse scattering from neutron [8] and X-ray [9] experiments, and hysteresis effects that extend far beyond the transition region, as seen in resistivity measurements along the thermal hysteresis loop [10]. These effects have been largely ignored, though one of the surface Fermi arcs has been noted to persist to ~ 90 K above the transition temperature and to have a history-dependent appearance [6]. More generally, structural phase transitions that involve in-plane translations of layers resulting from changes in temperature or pressure have been neglected, but many materials belong to this group, including Ta_2NiSe_5 [11], In_2Se_3 [12, 13], $\alpha\text{-RuCl}_3$ [14], CrX_3 ($X=\text{Cl, Br, I}$) [15], and MoS_2 [16–18]. A better understanding of these types of transitions would not only elucidate these material properties, but could also lead to the discovery of new phases.

The T_d and $1T'$ phases can be constructed from a stacking pattern of “A” and “B” operations, as shown in

Fig. 1(a). The A operation maps one layer of T_d to the layer below it, so T_d can be built from repeating “AA” sequences. The B operation is A followed by a translation by ± 0.15 lattice units, with the sign alternating layer-by-layer. Thus, $1T'$ can be built from repeating “AB” sequences. Diffuse scattering observed in the $H0L$ scattering plane on cooling from $1T'$ to T_d (in particular, the low intensity along $(60L)$) is consistent with a disordered A/B stacking pattern [8]. How the stacking changes with temperature has not been closely examined, though an explanation for the relative stability of the T_d and $1T'$ phases via free energy calculations was earlier proposed [19]. Understanding the nature of layer stacking will provide useful insight into how Weyl nodes disappear across the phase boundary.

We performed elastic neutron scattering to study the mechanism of the structural phase transition between the $1T'$ and T_d phases in MoTe_2 . On warming, we observed a new crystal phase, with a pseudo-orthorhombic structure and a four-layer unit cell, rather than the two-layer unit cells of $1T'$ and T_d phases. We refer to this new phase as T_d^* . The stacking sequence of T_d^* can be described by “AABB”, as shown in Fig. 1(a). Upon warming, the $T_d \rightarrow T_d^*$ transition is not accompanied by disorder, but diffuse scattering is seen on further warming from T_d^* to $1T'$. On the other hand, on cooling from $1T'$ to T_d , the T_d^* phase is absent and only diffuse scattering is observed instead, suggesting a frustrated tendency toward the “AABB” layer order.

Elastic neutron scattering was performed at Oak Ridge National Laboratory, on the triple axis spectrometers HB1, CG4C, and HB1A at the High Flux Isotope Reactor; and on the time-of-flight spectrometer CORELLI at the Spallation Neutron Source [20]. Though the crystals are monoclinic at room temperature, for simplicity, we use orthorhombic coordinates, with $a \approx 6.3$ Å and $c \approx 13.8$ Å. The collimations were $48'-40'-S-40'-120'$ for HB1 and CG4C, and $40'-40'-S-40'-80'$ for HB1A. Incident neutron energies were 13.5 meV for HB1, 4.5 meV for CG4C, and 14.6 meV for HB1A. Resistance measure-

* Present address: Duke University, Dept. of Physics, Durham, NC 27708

† Corresponding author. Email: louca@virginia.edu

ments were performed in a Quantum Design Physical Property Measurement System.

MoTe₂ crystals were grown in excess Te flux, including two used for neutron scattering, labeled “MT1” and “MT2”, and two used for resistance measurements. Details can be found in the Supplemental Materials.

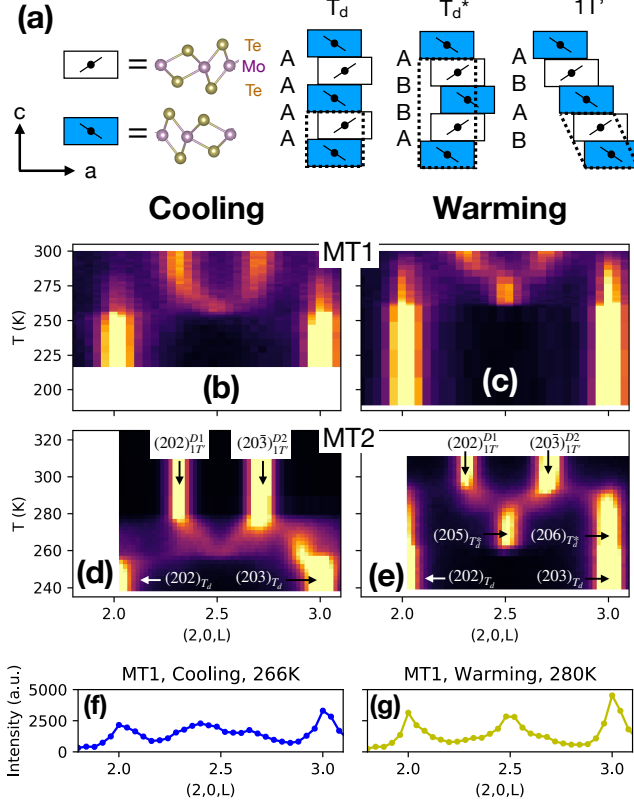


Figure 1. (a) The stacking patterns of 1T', T_d^{*}, and T_d. Rectangles show cells centered on points of inversion symmetry for each layer. Neutron scattering intensity maps for (b,c) MT1 and (d,e) MT2 as a function of temperature along the (2, 0, L) line on cooling (left) and warming (right). Data were taken on HB1A for (b,c) and HB1 for (d,e). (f,g) Intensity plots along (2, 0, L) showing diffuse scattering in MT1 on cooling (f) and warming (g).

In Figures 1(b-e), neutron scattering intensity scans along (2, 0, L) are combined for many temperatures on cooling and warming through the hysteresis. Figures 1(f) and 1(g) show individual scans. At low temperatures, T_d-phase Bragg peaks at $L = 2$ and $L = 3$ are observed. On warming from the T_d phase past ~ 260 K, a peak appears at $L = 2.5$, indicating the onset of the T_d^{*} phase. The presence of this peak at half-integer L indicates an out-of-plane doubling of the unit cell, so we label this peak $(205)_{T_d^*}$. With additional warming, a gradual transformation into the 1T' phase occurs, accompanied by diffuse scattering indicating stacking disorder. In the 1T' phase, the $(202)_{1T'}$ and $(203)_{1T'}$ Bragg peaks are observed near $L = 2.3$ and $L = 2.7$, respectively; D1 and

D2 denote each of the two 1T' twins. (Since MT1 could not be warmed fully into 1T' in Fig. 1(c) for technical reasons, diffuse scattering was present on subsequent cooling from 300 K in Fig. 1(b).) On cooling from the 1T' phase, no clear peak is seen near $L = 2.5$. Instead, intensity remains diffuse as it shifts toward (2,0,2.5). For MT2, we measured through the hysteresis twice and found the same patterns of diffuse scattering at the same temperatures along the hysteresis, suggesting that changes in diffuse scattering through the hysteresis are reproducible.

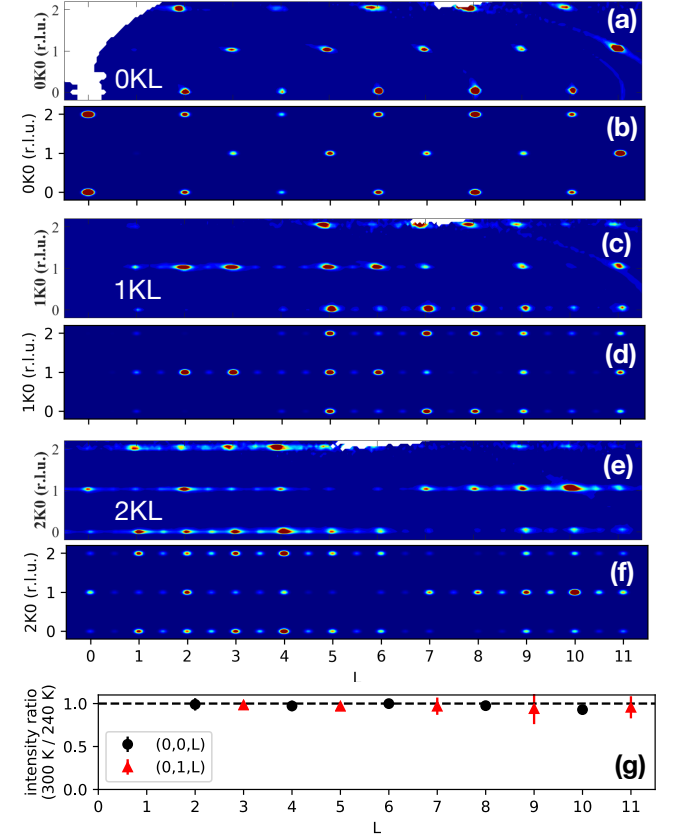


Figure 2. Neutron scattering intensity maps (a,c,e) and simulated data (b,d,f) in the 0KL (a,b), 1KL (c,d), and 2KL (e,f) scattering planes, from the MT1 crystal measured at CORELLI. Data taken on warming at 300 K. (g) Ratio of 0KL plane Bragg peak intensities between 300 K and 240 K.

We deduce the T_d^{*} phase structure from the following observations: First, T_d^{*} appears to be orthorhombic, but has additional peaks at half-integer L relative to T_d, indicating an out-of-plane doubling of the unit cell. Second, as noted above, sequences of A/B stacking operations can be used to describe the 1T' and T_d phases. There are only two A/B sequences that produce a pseudo-orthorhombic phase with a four-layer unit cell, “AABB” and “ABBA”, which are twins of each other. Since this structure, with highest possible symmetry P2₁/m, is incompatible with orthorhombic space groups, we refer to it as pseudo-orthorhombic.

To determine whether the T_d^* phase has the predicted AABB stacking, we carried out single-crystal neutron diffraction measurements on the MT1 crystal on CORELLI, with data shown in Figures 2(a,c,e). The data were taken on warming to 300 K, and the presence of peaks at half-integer L in the $2KL$ plane in Fig. 2(e) indicate the presence of the T_d^* phase. (The temperature discrepancy between the detection of T_d^* at 300 K on CORELLI and up to ~ 280 K on HB1A was likely due to a systematic error in temperature measurement between these sample environments.) The diffuse scattering streaks along L are from stacking disorder that was present on warming from 240 K, possibly due to a previous incomplete transition into T_d . Figures 2(b,d,f) show simulated intensity maps. To match the data, it was necessary to account for a 47.8% volume fraction of T_d as well as 28.2% and 24.0% volume fractions of the two T_d^* twins. The volume fractions were obtained by fitting the intensities of the Bragg peaks within $-1 \leq H \leq 8$, $-1 \leq K \leq 1$, and $-20 \leq L \leq 20$ with the calculated peak intensities of the ideal “AA”, “AABB”, and “ABBA” stacking sequences of T_d and the two T_d^* twins, respectively. These structures were built from layers having the coordinates in Ref. [21]. As can be seen in Figures 2(a-f), the patterns of peak intensities in these scattering planes match those arising from our model.

The $0KL$ plane Bragg peak intensities in Fig. 2(a), taken in the T_d^* phase, differ little from the $0KL$ plane intensities in $1T'$ or T_d [8]. In fact, ratios of $0KL$ peak intensities between data at 300 K and 240 K (in the T_d phase) are close to unity, as seen in Fig. 2(g). Since $0KL$ plane intensities are sensitive only to position along the b - or c -directions, the lack of change in $0KL$ intensities is consistent with T_d^* having AABB-type stacking, which differs from the $1T'$ or T_d structures by layer displacements along the a -direction. Based on the lack of significant change in position along the b - or c -directions, and the similarity between our data and simulations, we conclude that AABB stacking describes the T_d^* phase. As for the AB-stacked $1T'$ phase, the AABB structure can be centrosymmetric, with $P2_1/m$ symmetry; inversion symmetry centers for the AABB structure are depicted in Fig. S1 in the Supplemental Materials. Barring small non-centrosymmetric distortions, which are unlikely given that first-principles calculations have shown that MoTe_2 layers isolated from the non-centrosymmetric T_d environment nevertheless tend to become centrosymmetric [22], we conclude that T_d^* is centrosymmetric with $P2_1/m$ symmetry. A structural refinement assuming $P2_1/m$ symmetry was performed (see Supplementary Materials), with rough agreement between the refined and ideal coordinates, though the absence of visible $0KL$ peaks in our data (apart from those with even $K+L$) indicates that the true T_d^* structure is closer to the ideal AABB stacking than our refined coordinates.

For a closer look at how the transition proceeds, in Fig. 3(a,b) we plot Bragg peak intensities as a function of tem-

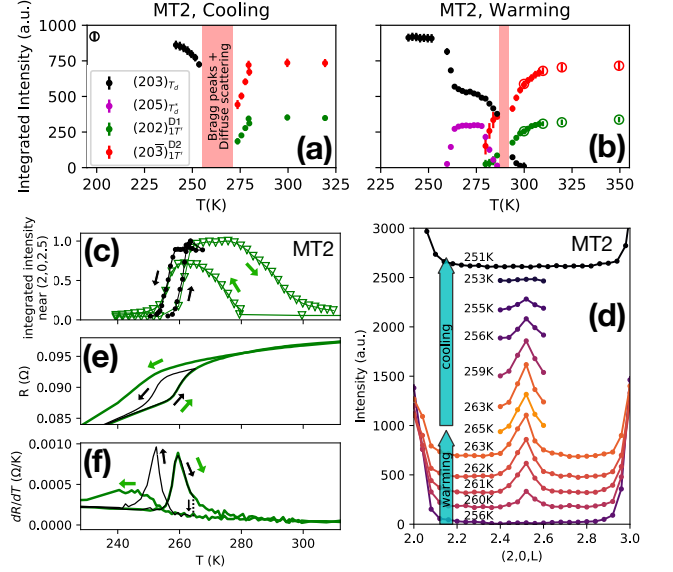


Figure 3. (a,b) Bragg peak intensities plotted as a function of temperature on warming and cooling for MT2. Red bands denote regions where fitting was poor. Closed symbols denote fits to the same hysteresis loop (with cooling data measured before warming). Open symbols correspond to a previous hysteresis loop. (c) Plots of intensity integrated within $(2, 0, 2.39 \leq L \leq 2.61)$ for MT2 taken through two different hysteresis loops. Data taken on CG4C for the narrow hysteresis (black), and on HB1 for the wide hysteresis (green; from same data as Fig. 1(d,e).) Curves normalized to their largest values. (d) Neutron scattering intensity along $(2, 0, L)$ for MT2, with data taken on CG4C at various temperatures, vertically displaced for clarity. (e) Resistance of a MoTe_2 crystal, measured through two hysteresis loops that begin on warming from 200 K. (f) The derivative dR/dT of the data shown in (e).

perature. The integrated intensities were obtained from fits of peaks present in intensity vs. the same $(2, 0, L)$ scans used for Figures 1(d) and 1(e). As we cool or warm to the extremes of the temperature range, there is a gradual increase in the intensity of the T_d and $1T'$ peaks. This increase occurs while the diffuse scattering decreases, as seen in Fig. S2 in the Supplemental Materials. However, the diffuse scattering at the temperature extremes of our measurements never completely disappeared. This lingering diffuse scattering is probably related to the long residual hysteresis commonly observed in resistivity measurements (e.g., in Ref. [23], or Fig. S3 in the Supplemental Materials.)

In contrast, as we cool or warm away from the extremes, the intensities of the $1T'$ and T_d peaks in Fig. 3(a) and 3(b) stay constant until a sudden change occurs. For instance, although the $1T' \rightarrow T_d$ transition proceeds with disorder on cooling, the decrease in $1T'$ peak intensities begins abruptly at ~ 280 K. On warming, the $(205)_{T_d^*}$ peak intensity also decreases around 280 K, sug-

gesting that 280 K marks a boundary between a tendency to favor either $1T'$ or T_d^* . Though T_d^* only appears on warming, the intensity shift toward (2,0,2.5) on cooling in Fig. 1(b) and 1(d) suggests a frustrated tendency toward the AABB stacking.

To investigate the boundary between the T_d and T_d^* regions, in Fig. 3(c), intensity integrated near (2,0,2.5) is plotted for two different thermal hysteresis loops for the MT2 crystal. The narrow hysteresis loop (black) warms into T_d^* , then cools back to T_d . Fig. 3(d) shows the data used to calculate the narrow hysteresis loop intensities; we see that the $(205)_{T_d^*}$ peak intensity rises and falls through the hysteresis loop, and that diffuse scattering is not present a few Kelvin below this peak's disappearance on cooling. Thus, $T_d^* \rightarrow T_d$ likely proceeds without disorder. In contrast, in the wide hysteresis loop (green), substantial diffuse scattering is present on cooling, as seen in Fig. 1(d,e). Nevertheless, for both narrow and wide hysteresis loops, a sudden drop of intensity near (2,0,2.5) appears on cooling below 255 K, though more gradually for the wide hysteresis loop.

A similar pattern can be seen in the resistance data in Fig. 3(e), taken on a MoTe_2 crystal with residual resistance ratio ~ 460 through consecutive narrow (black; 200 to 265 K) and wide (green; 200 to 350 K) hysteresis loops. On cooling, the resistance decreases quickly and in a symmetric manner (for cooling vs. warming) for the narrow hysteresis loop, but more slowly and asymmetric for the wide hysteresis loop. Even so, the temperature at which both loops begin to bend on cooling is similar, as seen from dR/dT in Fig. 3(f), though slightly lower for the wide hysteresis loop. The kink seen on warming (near 258 K) is likely the onset of T_d^* and not $1T'$, judging from the temperature and the similarities between the resistance and neutron scattering hysteresis loops.

We now discuss how these structural transitions proceed and the kinds of interlayer interactions that may be responsible, beginning from the observation that the onset to T_d occurs at a similar temperature whether cooling from the ordered T_d^* phase, or from the frustrated T_d^* region accessed on cooling from $1T'$. Since the onset temperature to T_d does not appear to vary substantially with overall stacking disorder, we suggest that *short-range* rather than long-range interlayer interactions determine the onset temperatures (into $1T'$ or T_d^* as well as T_d). (Though we use the term “interlayer interactions”, we emphasize that these are effective interactions. Whether an interlayer boundary shifts from A \rightarrow B depends on the free energy, which depends on the surrounding environment, which is specified by the A/B stacking sequence. “Interlayer interactions” represent the dependence of an interlayer boundary’s contribution to the free energy on the surrounding stacking, and can be indirect, involving changes to band structure, phonon dispersion, etc.)

In contrast, *long-range* interlayer interactions may govern the gradual decrease in diffuse scattering and increase in Bragg peak intensities on warming into $1T'$

or cooling into T_d . What kind of stacking faults causing this diffuse scattering persist on, say, cooling into T_d , even when short-range interlayer interactions favor an ordered phase? At twin boundaries, shifts of A \rightarrow B or B \rightarrow A (e.g., AAAABBB... \rightarrow AAABBBB...) would not change the short-range environment, and could only be induced by changes in long-range interlayer interactions. The decrease in diffuse scattering in T_d on cooling can be explained by the annihilation of these twin boundaries, either by joining in pairs or by exiting a crystal surface. The lack of change on subsequent warming can be explained by the relaxation of conditions that, on cooling, had driven twin boundaries to annihilate.

Previous studies on MoTe_2 should be re-examined in light of the existence of the T_d^* phase. First, the hysteresis loop in resistivity (first reported in Ref. [24]) has been interpreted as indicating the transition between T_d and $1T'$, but in view of the current data, most of the change in the resistance occurs between T_d and T_d^* on warming. Second, second harmonic generation (SHG) intensity measurements, expected to be zero for inversion symmetry and nonzero otherwise, show abrupt (within <4 K) changes on both heating and cooling through the hysteresis loop [25]. Since the transition to $1T'$ occurs gradually, and since T_d^* appears to be centrosymmetric, we suggest that the abrupt warming transition seen in SHG may be due to the $T_d \rightarrow T_d^*$ rather than $T_d \rightarrow 1T'$ transition. The abrupt transition on cooling is harder to explain, but it is possible that the loss of inversion symmetry on cooling into T_d occurs suddenly even as the transition proceeds with disorder. Our findings may also inform proposed applications, such as the photoinduced ultrafast topological switch in Ref. [26]; since the $T_d \rightarrow T_d^* \rightarrow T_d$ transition occurs without disorder and with only a ~ 5 K hysteresis, and since T_d^* appears to be centrosymmetric, a topological switch may more efficiently use T_d^* rather than $1T'$.

In conclusion, elastic neutron scattering showed, for the first time, an intermediate phase in the T_d to $1T'$ transition in MoTe_2 . On warming from the orthorhombic T_d , the pseudo-orthorhombic T_d^* arises without diffuse scattering and corresponds to an “AABB” sequence of stacking operations. Diffuse scattering is present on further warming from T_d^* to $1T'$, and on cooling from $1T'$ to T_d . A frustrated tendency toward the “AABB” stacking is seen on cooling.

ACKNOWLEDGEMENTS

This work has been supported by the Department of Energy, Grant number DE-FG02-01ER45927. A portion of this research used resources at the High Flux Isotope Reactor and the Spallation Neutron Source, which are DOE Office of Science User Facilities operated by Oak Ridge National Laboratory.

- [1] Yan Sun, Shu-Chun Wu, Mazhar N Ali, Claudia Felser, and Binghai Yan, "Prediction of Weyl semimetal in orthorhombic MoTe_2 ," *Physical Review B* **92**, 161107(R) (2015).
- [2] Ke Deng, Guoliang Wan, Peng Deng, Kenan Zhang, Shijie Ding, Eryin Wang, Mingzhe Yan, Huaqing Huang, Hongyun Zhang, Zhilin Xu, *et al.*, "Experimental observation of topological Fermi arcs in type-II Weyl semimetal MoTe_2 ," *Nature Physics* **12**, 1105 (2016).
- [3] D. Rhodes, R. Schönemann, N. Aryal, Q. Zhou, Q. R. Zhang, E. Kampert, Y.-C. Chiu, Y. Lai, Y. Shimura, G. T. McCandless, J. Y. Chan, D. W. Paley, J. Lee, A. D. Finke, J. P. C. Ruff, S. Das, E. Manousakis, and L. Balicas, "Bulk Fermi surface of the Weyl type-II semimetallic candidate MoTe_2 ," *Physical Review B* **96**, 165134 (2017).
- [4] Qiong Zhou, D. Rhodes, Q. R. Zhang, S. Tang, R. Schönemann, and L. Balicas, "Hall effect within the colossal magnetoresistive semimetallic state of MoTe_2 ," *Physical Review B* **94**, 121101(R) (2016).
- [5] S. Thirupathaiah, Rajveer Jha, Banabir Pal, J. S. Matias, P. K. Das, P. K. Ravikumar, I. Vobornik, N. C. Plumb, M. Shi, R. A. Ribeiro, and D. D. Sarma, "MoTe₂: An uncompensated semimetal with extremely large magnetoresistance," *Physical Review B* **95**, 241105(R) (2017).
- [6] Andrew P. Weber, Philipp Rüßmann, Nan Xu, Stefan Muff, Mauro Fanciulli, Arnaud Magrez, Philippe Bugnon, Helmut Berger, Nicholas C. Plumb, Ming Shi, Stefan Blügel, Phivos Mavropoulos, and J. H. Dil, "Spin-Resolved Electronic Response to the Phase Transition in MoTe_2 ," *Physical Review Letters* **121**, 156401 (2018).
- [7] N. Xu, Z. W. Wang, A. Magrez, P. Bugnon, H. Berger, C. E. Matt, V. N. Strocov, N. C. Plumb, M. Radovic, E. Pomjakushina, K. Conder, J. H. Dil, J. Mesot, R. Yu, H. Ding, and M. Shi, "Evidence of a Coulomb-Interaction-Induced Lifshitz Transition and Robust Hybrid Weyl Semimetal in $T_d\text{-MoTe}_2$," *Physical Review Letters* **121**, 136401 (2018).
- [8] John A. Schneeloch, Chunruo Duan, Junjie Yang, Jun Liu, Xiaoping Wang, and Despina Louca, "Emergence of topologically protected states in the MoTe_2 Weyl semimetal with layer-stacking order," *Physical Review B* **99**, 161105(R) (2019).
- [9] R. Clarke, E. Marzella, and HP Hughes, "A low-temperature structural phase transition in $\beta\text{-MoTe}_2$," *Philosophical Magazine B* **38**, 121–126 (1978).
- [10] Thorsten Zandt, Helmut Dwelk, Christoph Janowitz, and Ricardo Manzke, "Quadratic temperature dependence up to 50 K of the resistivity of metallic MoTe_2 ," *Journal of Alloys and Compounds Proceedings of the 15th International Conference on Solid Compounds of Transition Elements*, **442**, 216–218 (2007).
- [11] A. Nakano, K. Sugawara, S. Tamura, N. Katayama, K. Matsubayashi, T. Okada, Y. Uwatoko, K. Munakata, A. Nakao, H. Sagayama, R. Kumai, K. Sugimoto, N. Maejima, A. Machida, T. Watanuki, and H. Sawa, "Pressure-induced coherent sliding-layer transition in the excitonic insulator Ta_2NiSe_5 ," *IUCrJ* **5** (2018), 10.1107/S2052252517018334.
- [12] Feng Ke, Cailong Liu, Yang Gao, Junkai Zhang, Dayong Tan, Yonghao Han, Yanzhang Ma, Jinfu Shu, Wenge Yang, Bin Chen, Ho-Kwang Mao, Xiao-Jia Chen, and Chunxiao Gao, "Interlayer-glide-driven isosymmetric phase transition in compressed In_2Se_3 ," *Applied Physics Letters* **104**, 212102 (2014).
- [13] Jinggeng Zhao and Liuxiang Yang, "Structure Evolutions and Metallic Transitions in In_2Se_3 Under High Pressure," *The Journal of Physical Chemistry C* **118**, 5445–5452 (2014).
- [14] A. Glamazda, P. Lemmens, S.-H. Do, Y. S. Kwon, and K.-Y. Choi, "Relation between Kitaev magnetism and structure in $\alpha\text{-RuCl}_3$," *Physical Review B* **95**, 174429 (2017).
- [15] Michael A. McGuire, Hemant Dixit, Valentino R. Cooper, and Brian C. Sales, "Coupling of Crystal Structure and Magnetism in the Layered, Ferromagnetic Insulator CrI_3 ," *Chemistry of Materials* **27**, 612–620 (2015).
- [16] Liliana Hromadová, Roman Martoňák, and Erio Tosatti, "Structure change, layer sliding, and metallization in high-pressure MoS_2 ," *Physical Review B* **87**, 144105 (2013).
- [17] Zhen-Hua Chi, Xiao-Miao Zhao, Haidong Zhang, Alexander F. Goncharov, Sergey S. Lobanov, Tomoko Kagayama, Masafumi Sakata, and Xiao-Jia Chen, "Pressure-Induced Metallization of Molybdenum Disulfide," *Physical Review Letters* **113**, 036802 (2014).
- [18] Avinash P. Nayak, Swastibrata Bhattacharyya, Jie Zhu, Jin Liu, Xiang Wu, Tribhuwan Pandey, Changqing Jin, Abhishek K. Singh, Deji Akinwande, and Jung-Fu Lin, "Pressure-induced semiconducting to metallic transition in multilayered molybdenum disulfide," *Nature Communications* **5**, 3731 (2014).
- [19] Hyun-Jung Kim, Seoung-Hun Kang, Ikutaro Hamada, and Young-Woo Son, "Origins of the structural phase transitions in MoTe_2 and WTe_2 ," *Physical Review B* **95**, 180101(R) (2017).
- [20] F. Ye, Y. Liu, R. Whitfield, R. Osborn, and S. Rosenkranz, "Implementation of cross correlation for energy discrimination on the time-of-flight spectrometer CORELLI," *Journal of Applied Crystallography* **51**, 315–322 (2018).
- [21] Yanpeng Qi, Pavel G. Naumov, Mazhar N. Ali, Catherine R. Rajamathi, Walter Schnelle, Oleg Barkalov, Michael Hanfland, Shu-Chun Wu, Chandra Shekhar, Yan Sun, Vicky Süß, Marcus Schmidt, Ulrich Schwarz, Eckhard Pippel, Peter Werner, Reinald Hillebrand, Tobias Förster, Erik Kampert, Stuart Parkin, R. J. Cava, Claudia Felser, Binghai Yan, and Sergey A. Medvedev, "Superconductivity in Weyl semimetal candidate MoTe_2 ," *Nature Communications* **7**, 11038 (2016).
- [22] Colin Heikes, I-Lin Liu, Tristin Metz, Chris Eckberg, Paul Neves, Yan Wu, Linda Hung, Phil Piccoli, Huibo Cao, Juscelino Leao, Johnpierre Paglione, Taner Yildirim, Nicholas P. Butch, and William Ratcliff, "Mechanical control of crystal symmetry and superconductivity in Weyl semimetal MoTe_2 ," *Physical Review Materials* **2**, 074202 (2018).
- [23] Thorsten Zandt, Helmut Dwelk, Christoph Janowitz, and Ricardo Manzke, "Quadratic temperature dependence up to 50 K of the resistivity of metallic MoTe_2 ," *Journal of alloys and compounds* **442**, 216–218 (2007).
- [24] H. P. Hughes and R. H. Friend, "Electrical resistivity anomaly in $\beta\text{-MoTe}_2$," *Journal of Physics C: Solid State*

- Physics **11**, L103 (1978).
- [25] Hideaki Sakai, Koji Ikeura, Mohammad Saeed Bahramy, Naoki Ogawa, Daisuke Hashizume, Jun Fujioka, Yoshinori Tokura, and Shintaro Ishiwata, “Critical enhancement of thermopower in a chemically tuned polar semimetal MoTe_2 ,” *Science Advances* **2**, e1601378 (2016).
- [26] M. Y. Zhang, Z. X. Wang, Y. N. Li, L. Y. Shi, D. Wu, T. Lin, S. J. Zhang, Y. Q. Liu, Q. M. Liu, J. Wang, T. Dong, and N. L. Wang, “Light-Induced Subpicosecond Lattice Symmetry Switch in MoTe_2 ,” *Physical Review X* **9**, 021036 (2019).